

Influence of the oxygen during the deposition of an indium tin oxide thin film by magnetron sputtering for heterojunction solar cells

© A.F. Ivanov^{1,2}, F.S. Egorov¹, N.D. Platonov², V.L. Matukhin², E.I. Terukov^{3,4}

¹ Hevel LLC,

429965 Novocheboksarsk, Russia

² Kazan State Power Engineering University,

420066 Kazan, Russia

³ Ioffe Institute,

194021 St. Petersburg, Russia

⁴ St. Petersburg State Electrotechnical University „LETI“,

197376 St. Petersburg, Russia

E-mail: ivanovaleksandr@yandex.ru; f.egorov@hevelsolar.com

Received September 27, 2021

Revised October 1, 2021

Accepted October 1, 2021

Optoelectronic properties of indium and tin oxide thin films depending on the oxygen content in the total gas flow were experimentally investigated during deposition of these films by DC magnetron target sputtering. Relationship of the heterojunction thin-film solar cell output parameters vs. oxygen partial pressure in a vacuum vessel was examined during indium and tin oxide layer deposition. The maximum photovoltaic conversion efficiency of the solar cell was achieved at an oxygen partial pressure in the vacuum vessel of ~ 6.5 Torr.

Keywords: heterojunction thin-film solar element, indium and tin oxide, magnetron sputtering.

DOI: 10.21883/SC.2022.03.53063.9747

1. Introduction

Transparent conductive oxides (TCO) are required as transparent electrodes for the manufacturing of modern photovoltaic converters (PVC). Due to their optoelectronic properties, indium tin oxide (ITO) transparent thin films are TCO widely used in this area [1]. Heterojunction with intrinsic thin-layer solar cells (HIT SC) on the *a*-Si:H thin-film amorphous silicon have already demonstrated high photovoltaic performance and have been recognized by now as one of the most advanced PVCs. The idea of the manufacturing process is to form heterojunctions on the surface of *c*-Si single-crystal silicon wafers by deposition of various types of *a*-Si:H amorphous silicon thin films [2–4]. HIT cells have high open-circuit voltage (V_{OC}) that is generally much higher than 730 mV, the world record in the current-voltage fill factor ($FF = 84.9\%$) and photovoltaic converter performance ($\eta = 26.7\%$) was set up by Kaneka Corp in 2017 [5]. In addition, *a*-Si:H thin films are deposited at $\sim 200^\circ\text{C}$, which significantly reduces the heat balance for solar cell production process while ensuring high performance of the equipment [2–5]. For the HIT cell architecture, a TCO layer shall be deposited on the front and rear sides of the solar cell to ensure efficient light transmission into the silicon device and to retain high specific conductivity [6–9].

Despite the high performance of HIT cells, some issues regarding the improvement of the production process for each individual cell structure layer are still remain open. They include some technical issues related to the

improvement of the TCO deposition process, since this step may definitely change the interface properties of the device structure and influence the output parameters of the finished SC. Magnetron sputtering is the most widely used TCO deposition process [10–12]. The optoelectronic properties of ITO thin films were reported to depend on the growth conditions, including the oxygen flow [13–15]. Some investigations show that the oxygen flow increase during deposition reduces the main charge carrier concentration and influences the ITO thin film bandgap width [13,14]. C.G. Choi et al. [15] have found that the ITO film transmittance in the visible range did not correlated with the oxygen flow, while Y.J. Kim et al. [10] have determined that both Hall mobility of main charge carriers and optical transmission of the film increase relative to the oxygen flow. Some differences in the obtained findings require additional investigations.

The purpose of the research was to investigate the influence of oxygen contained in the total gas flow during magnetron sputtering on the optical and electrophysical properties of ITO thin films. In addition, influence of the oxygen content in the vacuum vessel during magnetron sputtering of ITO thin films on the output parameters of the finished HIT cells was investigated.

2. Experimental procedure

Samples for investigation of the influence of oxygen contained in the total gas flow on the optical and electrophysical properties of ITO thin films were prepared

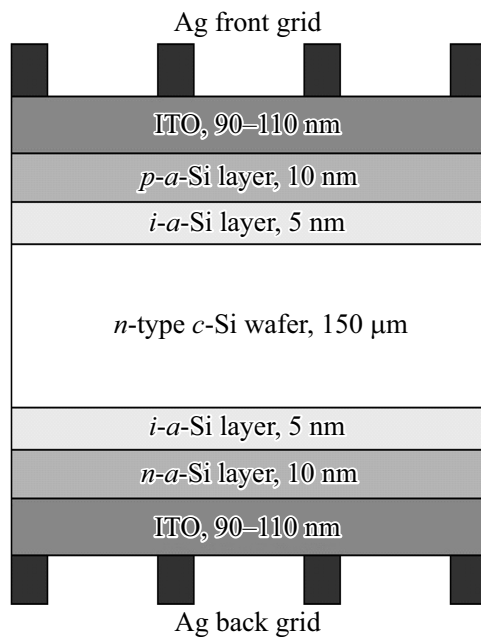


Figure 1. Schematic view of HIT cell.

by DC magnetron target sputtering ($\text{In}_2\text{O}_3 = 95\%$ and $\text{SnO}_2 = 5\%$). Sputtering was carried out at 200°C and vacuum vessel pressure max. $6 \cdot 10^{-3}$ mbar at various relationships of oxygen vs. total gas flow:

$$r(\text{O}_2) = \text{O}_2 / (\text{Ar} + \text{O}_2),$$

where O_2 is the oxygen flow during the magnetron sputtering of ITO thin film, Ar is the argon flow during the magnetron sputtering of ITO thin film. Direct current power density was 1.13 W/cm^2 , and $r(\text{O}_2) = 2.2 \cdot 10.4\%$. Film thickness (Thk) was measured by the ellipsometric method using AccuMap-SETM V-1500 spectroscopic ellipsometer. Surface resistivity (R) was measured by the four-probe method using JANDEL RM3-ARC system. Surface concentration (n) and Hall mobility (μ) of the main charge carriers were measured using HMS-3000 system. Each of the samples was measured several times: in 4–5 various positions (after each measurement on HMS-3000 system, the sample was rotated at 90°). The total measurement result is given as the average value from 4–5 measurements. Optical transmission (t) and reflection (r) of films were measured using Perkin Elmer Lambda 950 spectrometer with integrating sphere, and absorbance (a) was calculated as $a = 100\% - t - r$.

For investigation of the oxygen content influence in the vacuum vessel during magnetron sputtering of ITO thin films on the HIT cell output parameters, SC were prepared from high quality n -type c -Si wafers. The HIT cell diagram is shown in Fig. 1. The wafers were preliminary subjected to pyramidal texturizing in alkali solution, chemical treatment and placed in fluoric acid before plasma-chemical vapor deposition of a -Si:H intrinsic and doped layers. ITO films

were used as front and rear electrodes and deposited by DC magnetron sputtering of ITO target ($\text{In}_2\text{O}_3 = 95\%$ and $\text{SnO}_2 = 5\%$) at 200°C and vacuum vessel pressure max. 10^{-2} mbar. The DC power surface density was 2.08 W/cm^2 , and oxygen partial pressure (P_{O_2}) in vacuum vessel varied within $P_{\text{O}_2} = 4.5 \cdot 10^{-7} - 10^{-6}$ Torr. The ITO layer sputtering was followed by silver grid applied by screen printing and SC annealing during 40 min at 200°C .

Oxygen partial pressure in the vacuum vessel was detected using HIDEN HPR-30 A2 system with differential pumping systems and HALO 201 RC mass-spectrometer. Investigations of test sample output parameters were carried out using Pasan Spot^{LIGHT} Highcap solar radiation pulse simulator with Grid^{TOUCH} contact system developed by Pasan for parameter measurement of busbarless solar cells. Current-voltage characteristics (CVC) of HIT cells were measured in AM1.5G conditions (1000 W/m^2).

3. Experimental results

Electrophysical measurements of ITO samples are shown in the table. The obtained data was used to plot relationships of oxygen content in the total gas flow $r(\text{O}_2)$ vs. surface concentration, Hall mobility of the main charge carriers and surface resistivity of the ITO test samples (Figs. 2–4).

The surface concentration and Hall mobility of the main charge carriers of ITO films were measured using Van der Pauw four-probe method. In addition, the electrodes contacted with the angles of the test ITO film that had a 1×1 cm square shape. Thus, the electrical properties of ITO layers were measured relative to $r(\text{O}_2)$. Surface concentration of the main charge carriers varied from $n = -3.777 \cdot 10^{20}$ to $-1.019 \cdot 10^{20} \text{ cm}^{-3}$ with the change in $r(\text{O}_2)$ from 2.2 to 10.4% (Fig. 2). For the whole test range of $r(\text{O}_2)$, Hall mobility of the main charge carriers varied from $\mu = 44.63$ to $23.29 \text{ cm}^2/\text{V} \cdot \text{s}$ (Fig. 2). Surface resistivity was increased in the range $R = 34.94 - 292.4 \ \Omega/\square$, with the change $r(\text{O}_2) = 2.2 - 10.4\%$ (Fig. 3).

At low surface concentration of the main charge carriers (n), the possible limiting factors for Hall mobility of the main charge carriers (μ) include carrier-ionized impurity and carrier-phonon scattering. However, at a higher electron

Electrophysical measurements of ITO samples

$r(\text{O}_2)$, %	Thk , nm	R , Ω/\square	μ , $\text{cm}^2/\text{V} \cdot \text{s}$	$n \cdot 10^{20}$, cm^{-3}
2.2	105.73	34.94	44.63	-3.777
3.3	97.29	41.96	48.73	-3.147
4.4	88.67	65.59	41.74	-2.562
5.2	106.73	36.57	43.33	-3.681
5.5	103.31	95.66	35.29	-1.795
7.6	94.41	86.9	39.42	-1.939
10.4	90.28	292.4	23.29	-1.019

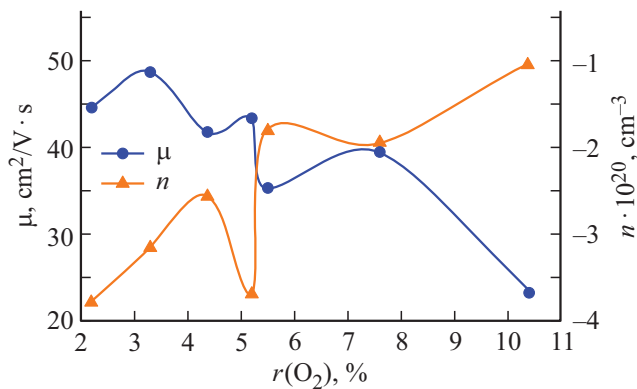


Figure 2. Hall mobility (μ) and surface concentration (n) of the main charge carriers vs. oxygen content in the total gas flow $r(\text{O}_2)$ during ITO thin film sputtering.

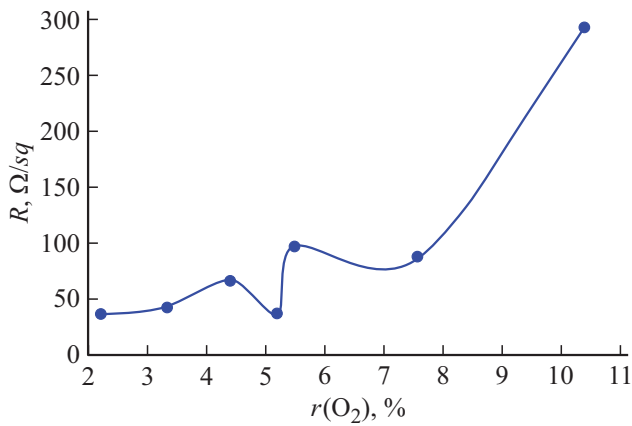


Figure 3. ITO film surface resistance (R) vs. oxygen content in the total gas flow $r(\text{O}_2)$ during ITO thin film sputtering.

concentration n , ionized impurity scattering is the main limiting factor for mobility μ [16,17]. The main charge carrier mobility achieves its maximum value, when the carrier transport was predominantly limited by electron-phonon interaction and ionized impurity loss had no effect on μ [17].

Figure 4 shows ITO film transmittance vs. absorbance at various $r(\text{O}_2)$. Samples with $n = -3.777 \cdot 10^{20}$ and $-3.681 \cdot 10^{20} \text{ cm}^{-3}$ have low absorbance in the visible and near-infrared (NIR) spectra. In the near-ultraviolet (NUV) band, Burstein–Moss shift may be also observed (i.e. absorption edge shift with increase in n at decrease in $r(\text{O}_2)$).

Optical absorption of films in the near IR band was found to increase significantly at $r(\text{O}_2) = 2.2$ and 5.2% , that could be associated with the increase in n measured using Hall effect (Fig. 1). It shall be noted that the ITO thin film applied at $r(\text{O}_2) = 5.2\%$ shows higher absorbance in the visible band as compared with the remaining samples.

Investigation of the influence of the oxygen content in the vacuum vessel during magnetron sputtering of ITO thin films on the HIT cell output parameters are shown in Figs. 5 and 6. Despite the oxygen partial pressure (P_{O_2}) during ITO layer sputtering, high V_{OC} was observed on a regular basis for all HIT cells which is indicative of the efficiency of the hydrogenated passivation of amorphous layers. With the increase in P_{O_2} , short circuit currents (I_{SC}) and photovoltaic conversion performance (η) of HIT cells were also increased. However, at $P_{\text{O}_2} > 6.22 \cdot 10^{-7}$ Torr, linear growth I_{SC} stopped as a result of resistive loss in the ITO layer. Since with the increase in P_{O_2} , FF decreased linearly (trend line FF), and linear growth I_{SC} stopped at

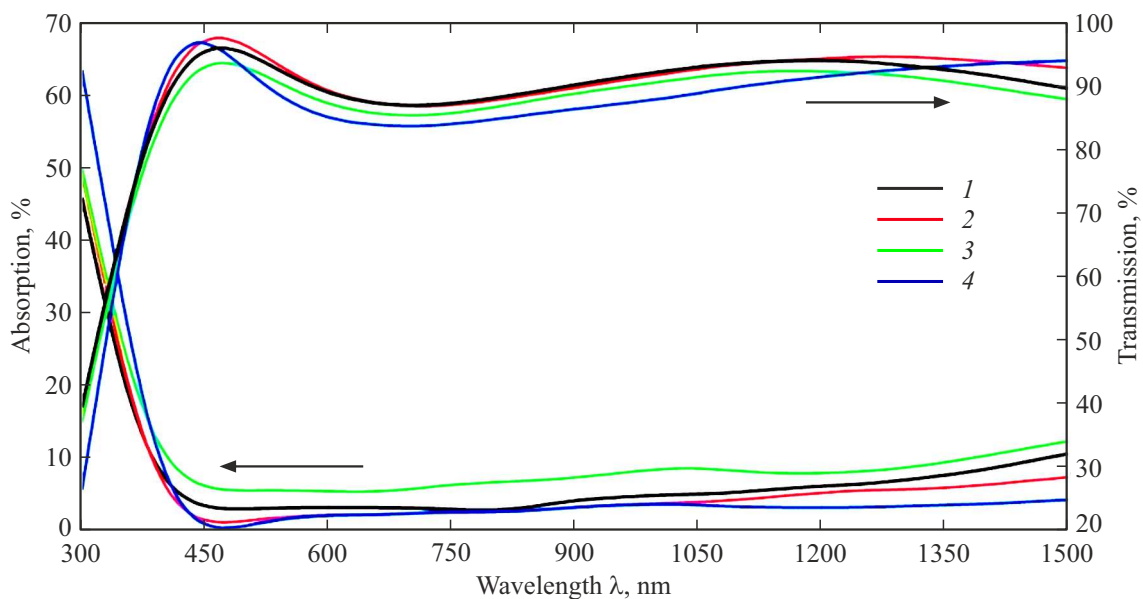


Figure 4. ITO film absorbance and transmittance vs. oxygen content in the total gas flow during ITO thin film sputtering, $r(\text{O}_2)$ in %: 2.2 (1), 3.3 (2), 5.2 (3), 10.4 (4). (Colored version of the figure is presented in electronic version of the article).

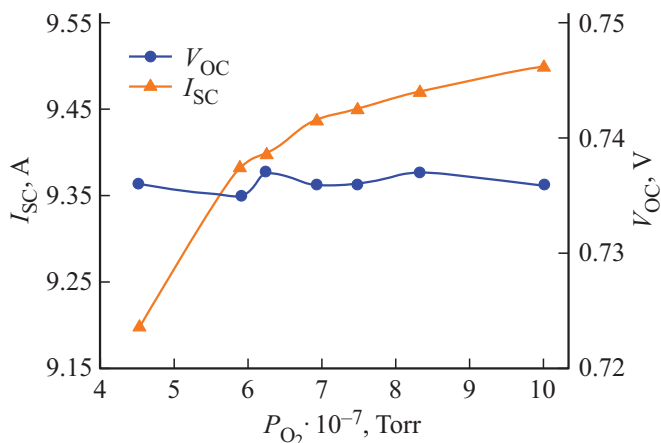


Figure 5. HIT cell short circuit current (I_{SC}) and idle voltage (V_{OC}) vs. oxygen partial pressure in the vacuum vessel during the magnetron sputtering of ITO thin film.

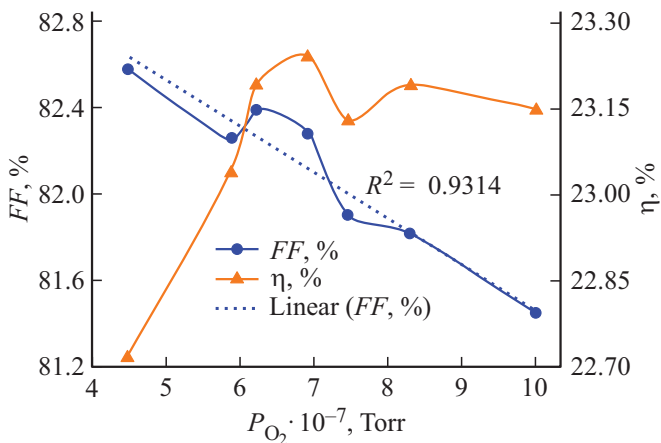


Figure 6. CVC fill factor (FF) and photovoltaic converter performance (η) of HIT cell vs. oxygen partial pressure in the vacuum vessel during the magnetron sputtering of ITO thin film.

$P_{O_2} > 6.22 \cdot 10^{-7}$ Torr, then η of HIT cells also did not increase any longer.

4. Conclusion

The research findings have shown the influence of oxygen contained in the total gas flow on the optical and electrophysical properties of ITO thin films, as well as the influence of the oxygen partial pressure in the vacuum vessel during magnetron sputtering of ITO thin film on the HIT cell output parameters. All ITO films with $r(O_2) > 5.2\%$ have shown low absorption in the visible and near IR spectra, and optical absorption of films in the near IR band increased dramatically with a decrease in the oxygen content that could be due to the increase in the surface concentration of the main charge carriers which, in its turn, was confirmed by the Hall effect measurement. Minimum surface resistivity and surface concentration of

the main charge carriers were achieved at the lowest $r(O_2)$. With the increase in the oxygen content in the total gas flow during ITO thin film sputtering, Hall mobility of the main charge carriers decreased and the minimum mobility of the main carriers achieved for ITO films was equal to $23 \text{ cm}^2/\text{V} \cdot \text{s}$. In addition, it was found that, when ITO were used as front and rear contacts in HIT cells, high photovoltaic conversion performance was achieved at the oxygen partial pressure in vacuum vessel ~ 6.5 Torr, which can be explained by optimum optical and electrophysical parameters of the ITO film. Low-temperature deposition and excellent optical and electrophysical properties of the ITO film demonstrate that ITO is one of the best potential transparent conductive electrode not only for solar cells, but also for many temperature sensitive devices such as organic LEDs and perovskite-based solar cells.

Conflict of interest

The authors declare that they have no conflict of interest.

References

- [1] B.G. Lewis, D.C. Paine. MRS Bull., **25** (8), 22 (2000).
- [2] S.Q. Xiao, S. Xu, H.P. Zhou, D.Y. Wei, S.Y. Huang, L.X. Xu, C.C. Sern, Y.N. Guo, S. Khan. Appl. Phys. Lett., **100** (23), 233902 (2012).
- [3] J. Haschke, O. Dupré, M. Boccard, C. Ballif. Sol. Energy Mater. Sol. Cells, **187**, 140 (2018).
- [4] E.I. Terukov, A.S. Abramov, D.A. Andronnikov, K.V. Emtsev, I.E. Panaiottoy, A.S. Titov, G.G. Shelopin. FTP, **52** (7), 792 (2018) (in Russian).
- [5] K. Yoshikawa, H. Kawasaki, W. Yoshida, T. Irie, K. Konishi, K. Nakano, T. Uto, D. Adachi, M. Kanematsu, H. Uzu, K. Yamamoto. Nature Energy, **2** (5), 17032 (2017).
- [6] Z.C. Holman, M. Filipič, A. Descoedres, S. De Wolf, F. Smole, M. Topič, C. Ballif. J. Appl. Phys., **113**, 013107 (2013).
- [7] L. Korte, E. Conrad, H. Angermann, R. Stangl, M. Schmidt. Sol. Energy Mater. Sol. Cells, **93** (6), 905 (2009).
- [8] K. Ji, J. Choi, H. Yang, H. Lee, D. Kim. Sol. Energy Mater. Sol. Cells, **95** (1), 203 (2011).
- [9] Y.J. Kim, S.B. Jin, S.I. Kim, Y.S. Choi, I.S. Choi, J.G. Han. Thin Sol. Films, **518** (22), 6241 (2010).
- [10] B. Zhang, X. Dong, X. Xu, P. Zhao, J. Wu. Sol. Energy Mater. Sol. Cells, **92** (10), 1224 (2008).
- [11] A. Thøgersen, M. Rein, E. Monakhov, J. Mayandi, S. Diplas. J. Appl. Phys., **109** (11), 113532 (2011).
- [12] S. Li, X. Qiao, J. Chen. Mater. Chem. Phys., **98** (1), 144 (2006).
- [13] M.-C. Chen, S.-A. Chen. Thin Sol. Films, **517** (8), 2708 (2009).
- [14] C.G. Choi, K. No, W.-J. Lee, H.-G. Kim, S.O. Jung, W.J. Lee, W.S. Kim, S.J. Kim, C. Yoon. Thin Sol. Films, **258** (2), 274 (1995).
- [15] H. Hosono. J. Non-Cryst. Solids, **352**, 851 (2006).
- [16] R. Martins, P. Almeida, P. Barquinha, L. Pereira, A. Pimentel, I. Ferreira, E. Fortunato. J. Non-Cryst. Sol., **352**, 1471 (2006).
- [17] A.J. Leenheer, A.J. Leenheer, J.D. Perkins, M.F.A.M. van Hest, J.J. Berry, R.P. O'Hayre, D.S. Ginley. Phys. Rev. B, **7**, 115215 (2008).